Abundances of the Rare-Earth Nuclei Produced by Rapid Neutron Capture in Supernovae*

ROBERT A. BECKER† AND WILLIAM A. FOWLER
Kellogg Radiation Laboratory, California Institute of Technology, Pasadena, California
(Received April 16, 1959)

Calculations have been carried out, following the method of Burbidge, Burbidge, Fowler, and Hoyle, for the abundances of nuclei in the rare-earth region which are produced in the rapid neutron-capture process thought to occur in supernovae. The recently available rare-earth mass differences of Johnson and Bhanot were employed. The calculated abundances agree, in general, with those given by Suess and Urey. The results of the computations support the work of Burbidge, Burbidge, Fowler, and Hoyle which showed the effect of spheroidal deformation above the closed shell at $N=126$ in enhancing the production of Th^{232}, U^{235}, U^{238}, Cf^{254}, etc., in supernovae. The effect of different combinations of temperature and neutron density in enhancing certain relative abundances is discussed briefly.

INTRODUCTION

BURBIDGE, Burbidge, Fowler, and Hoyle[1] (BBFH) have given a detailed analysis of element synthesis involving a variety of processes believed to take place in stars. General agreement was found between computed abundances and those given in the survey of Suess and Urey[2] (SU). According to BBFH, the heavy nuclei beyond the iron group are thought to be produced mainly by neutron capture, two distinct processes being involved which differ widely in respect to the time scale and neutron flux involved. The slow (s) process, characterized by a low neutron flux, is believed to take place in second-generation red giant stars on a time scale such that 10^2 to 10^4 years may elapse between successive neutron captures in a single chain. (By "second generation" we imply only that the star already contains elements up to the iron group which were produced in the first-generation stars of the galaxy.) The rapid (r) process, on the other hand, is thought to take place during the initial phases of the supernova-type explosion of a second-generation star. In the first 10^2 to 10^3 seconds of a supernova event, an intense flux of neutrons is assumed to be present. BBFH estimate that a flux of $\sim 10^{32}$ neutrons per cm^2 per second at a temperature of $\sim 10^9$ degrees Kelvin occurred in the supernova event which gave birth to the solar system abundances. The origin of the neutrons is considered to be α-particle capture by certain nuclei, such as Ne^{21}, which had previously been produced in the NeNa-cycle in the hydrogen-burning core of the second-generation star while it was still on the main sequence, or alternatively in the hydrogen-burning shell during the red-giant stage. The r process is pictured as a competition between two types of event: on the one hand, rapidly occurring successive captures of neutrons, and, on the other hand, photoejection of the neutrons in the intense bath of heat radiation present during the explosion. Under these conditions, successive neutron captures produce neutron-rich nuclei far to the electron-unstable side of the stable isobars. As the neutron flux dies down, the neutron-rich nuclei decay back to the stability region through repeated negative beta decays.

The rapid process, together with other nuclear reactions involved in stellar nuclear synthesis, is described in detail in the review article by BBFH. Since the writing of that paper, accurate neutron binding energies have become available for the stable nuclei in the range of atomic weights from 140 to 200, chiefly through mass-spectroscopic measurements by Johnson and Bhanot.[3] Accordingly, the results of these two authors have been employed in the present work in order to determine the r-process progenitors of the elements in the rare-earth region and their abundances.

DETAILS OF THE CALCULATION

BBFH have given the critical neutron-binding energy in Mev, above which neutron capture will occur on the average, as

$$Q_n \gtrsim \frac{T_9}{5.04}(34.07+\tfrac{3}{2}\log T_9-\log n_n), \qquad (1)$$

where T_9 is the temperature in units of 10^9 degrees Kelvin, n_n is the density of neutrons, and the logarithms are to the base 10. For $T_9=1$ and $n_n=10^{24}/cm^3$, $Q_n \gtrsim 2.0$ Mev. In the present instance, a better fit with the rare-earth abundances of SU is obtained with the choice $Q_n \gtrsim 1.6$ Mev. This entails a slightly altered combination for the adjustable parameters T_9 and n_n, e.g., $n_n=10^{24}$, $T_9=0.8$. The determination of the neutron-capture path was carried out in the manner outlined by BBFH. In this treatment, a modified form of the Weizsäcker mass formula is used which takes into account such effects as those arising from closure of nuclear shells and from spheroidal deformation of

* Supported in part by the joint program of the Office of Naval Research and the U. S. Atomic Energy Commission.
† On leave from the University of Illinois. Partially supported by a grant from the Guggenheim Foundation.
[1] Burbidge, Burbidge, Fowler, and Hoyle, Revs. Modern Phys. **29**, 547 (1957). This paper is referred to hereinafter as BBFH.
[2] H. E. Suess and H. C. Urey, Revs. Modern Phys. **28**, 53 (1956). This paper is referred to hereinafter as SU.
[3] W. H. Johnson, Jr., and V. B. Bhanot, Phys. Rev. **107**, 1669 (1957).

the nuclear core between neutron shell closure at 82 and 126 neutrons, and beyond 126 neutrons. For a given neutron-rich nucleus, the neutron-binding energy is obtained from those known for the stable nuclei having the same number of neutrons. The assumption is made that neutron shell effects are a function only of the neutron number N, and that proton shell effects are a function only of the proton number Z. On this basis, it can be shown that the binding energy for the next added neutron to a nucleus (A,Z) is given by

$$Q_n(A,Z)\simeq[Q_n(A_e,Z_e)-4\beta Z_e^2/A_e^2]+4\beta Z^2/A^2-0.41, \quad (2)$$

where the subscript e pertains to a nucleus with known Q_n, and β is the coefficient of the isotopic asymmetry term in the Weizsäcker formula. The relation $N=A-Z=A_e-Z_e$ must hold. The last term in (2) is an approximation to various small terms which have been evaluated numerically. A knowledge of $Q_n(A,Z)$ permits the determination of the rapid-capture path once a critical Q_n for capture has been determined through the application of Eq. (1).

When equilibrium between the (n,γ) and (γ,n) processes is reached, further progress along the r-process path is made only through negative beta decay. Thus, the abundance of a nucleus produced by the r process will depend linearly on the beta-decay lifetime of its progenitor situated on the r-process path. This lifetime depends in turn on the energy available for the decay event. The beta-decay energies of the highly unstable progenitors are found by considering the mass parabolas of isobaric sequences, according to the formula

$$W=B_A(Z_A-Z-2.5)+0.5\begin{cases}+0, & A \text{ odd}, Z \text{ odd}\\ -\frac{1}{2}\delta_A, & A \text{ even}, Z \text{ even}\end{cases} \quad (3)$$

with all energies in Mev. Here Z_A is the charge of the hypothetically most stable nucleus in the isobaric sequence, and B_A is the curvature of the parabola at the vertex. Values for Z_A were determined empirically from known beta-decay energies. B_A values given by BBFH were employed. The term $\frac{1}{2}\delta_A$ is the pairing energy described in the same paper. The term $2.5B_A$ replaces the customary term $0.5B_A$ because the allowed beta-decay transitions will occur in general to a low excited state with excitation of the order of $2B_A$, rather than to the ground state of the residual nucleus. As before, the mean lifetime τ_β for beta decay, and the atomic abundance $n(A)$ are given by

$$\tau_\beta=(10^4/W_\beta^5)\text{ sec}, \quad (4)$$

and

$$n(A)=\text{const}(\tau_\beta/\Delta A), \quad (5)$$

where ΔA is the number of neutron captures made by the isobar of weight A before the next beta decay occurs. Expression (5) assumes that all of the material produced at a given mass number A at which beta decay occurs is spread out, at the termination of the supernova event, over an interval up to the next mass number, $A+\Delta A$, at which beta decay occurs. The numerical quantity in (4) is a very rough approximation for allowed beta-transitions over an extended range of mass numbers.

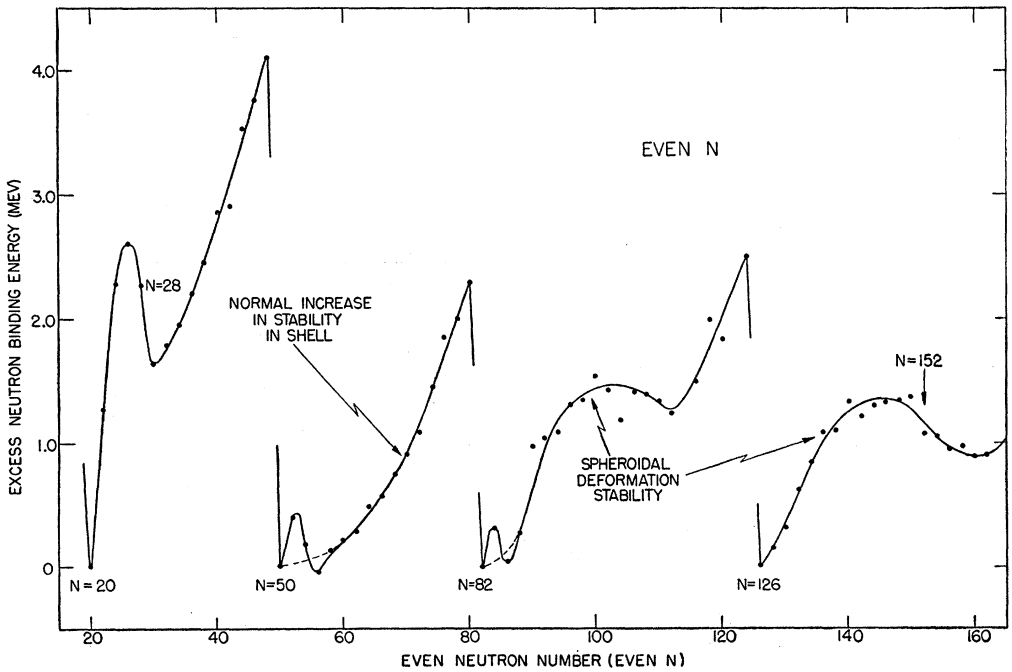

FIG. 1. The average excess neutron binding energy to nuclei with neutron number N, over that given by the smooth Weizsäcker atomic mass formula. Each value has been normalized to the value at the beginning of the shell in which N lies.

Relative abundances do not depend on the exact value of this constant.

As in the original article of BBFH, the atomic abundances $n(A)$ have been normalized to those of SU, taking the number of Te^{128} atoms as 1.48, which is in turn normalized to a standard value of 10^6 for silicon. However, we have multiplied the computed $n(A)$ by a factor of 2 in order to take into account the effect of cycling after spontaneous fission above $A=260$. Because the fission fragments peak at $A\simeq140$, the effect of cycling is such that the flow of nuclei above $A=140$ is twice as great as in the range of A from 110 to 140. This was not done in BBFH.

Figure 1 shows, for the next added neutron, the manner in which the binding energy excess over that given by the usual Weizsäcker formula increases experimentally with neutron number after shell closure at 20, 50, 82, and 126 neutrons for known nuclei. The curve for the region between 82 and 126 neutrons is deduced from the recent measurements of Johnson and Bhanot.[3] In the other regions, the masses of Huizenga[4] and Wapstra[5] have been used. The $N=20$ to 50 shell also exhibits the stability associated with the subshell at $N=28$. The $N=50$ to 82 shell shows the normal increase in stability within the shell as N increases, unperturbed by quadrupole spheroidal deformations.

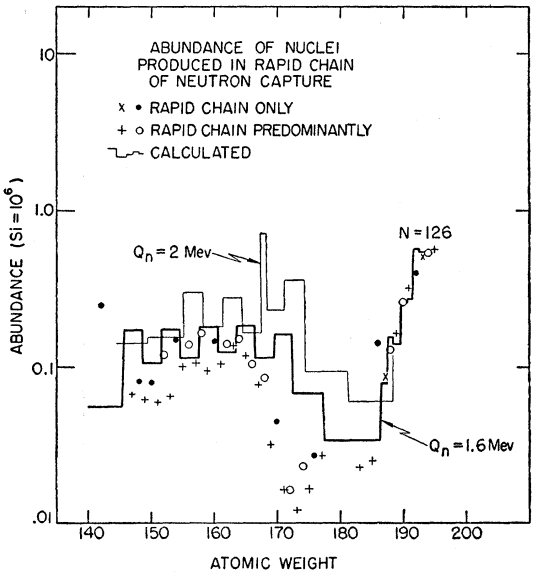

FIG. 2. Abundances of nuclei in the region of the rare earths which are produced in the r process. The empirical points are taken from SU.[2] The histogram is a curve calculated by the method more fully described in the work of BBFH.[1] The abundances are normalized to silicon taken as 10^6 atoms. The heavy line depicts the conditions believed to be responsible for the solar system abundances of these nuclei (Q_n critical=1.6 Mev).The light line shows the effect of increasing the temperature to 1.0×10^9 degrees (Q_n critical=2.0 Mev). Both situations are normalized to show a common abundance for an element like tellurium (not included in the diagram).

[4] J. R. Huizenga, Physica **21**, 410 (1955).
[5] A. H. Wapstra, Physica **21**, 367, 387 (1955).

Such deformations are known to be quite small in this shell. On the other hand, both the $N=82$ to 126 and the $N=126$ to 184 shells exhibit marked effects due to the large spheroidal deformations which are known to occur approximately midway in these shells. Large quadrupole moments are observed for nuclei in these regions.

It should be mentioned that the exact shapes of curves such as are given in Fig. 1 depend somewhat on the choice of the parameter β in the Weizsäcker formula. It was found, however, that the general character of the curves is preserved for not too large changes in β from the value of 22.6 Mev, given in BBFH.

RESULTS

Rare-Earth Abundances

The results of the calculations for the rare-earth region are shown in Table I. The critical value $Q_n=1.6$ Mev was chosen as the best fit to the SU abundance distribution. It is of interest to note that the sum of the decay times over the entire region of the rare-earth progenitors ($A\simeq141$ to 178) is about 1 second as compared with a total of about 80 seconds for one cycle of the entire r path.[1] Thus, the progenitors of the rare earths in one cycle build up a population of roughly 1% of all the r-process nuclei. Figure 2 displays a histogram of the calculated abundance distribution in the region of interest. Following the practice of BBFH, we present the calculated results in the form of a histogram rather than a smooth curve. In this way, the order of magnitude, but not the exact nature of fluctuations due to odd-even effects, etc., is indicated. SU abundances are indicated by the plotted points. The solid circles (even A) and crosses (odd A) represent neutron-rich *stable* nuclei, that is, they exist as stable

TABLE I. The path of the r-process and abundances in the rare-earth region.[a]

N	A	Z	Z_A	B_A Mev	$\frac{1}{2}\delta_A$ Mev	W_β Mev	τ_β sec	ΔA	Atomic abundance
92	141	49	60.0	1.29	···	11.47	0.0504	5	0.056
96	146	50	60.8	1.28	0.98	10.14	0.0933	3	0.172
98	149	51	61.9	1.27	···	11.17	0.0575	3	0.106
100	152	52	62.9	1.26	0.93	10.15	0.0928	3	0.172
102	155	53	63.9	1.25	···	11.00	0.0621	3	0.114
104	158	54	64.9	1.24	0.89	10.03	0.0985	3	0.182
106	161	55	65.9	1.23	···	10.83	0.0671	3	0.124
108	164	56	67.0	1.22	0.86	10.01	0.0995	3	0.184
110	167	57	68.1	1.22	···	10.99	0.0624	3	0.115
112	170	58	69.2	1.21	0.83	10.20	0.0906	3	0.164
114	173	59	70.6	1.21	···	11.51	0.0495	5	0.0686
118	178	60	72.2	1.19	0.80	11.24	0.0557	9	0.0340
126	187	61	75.6	1.18	···	14.78	0.0142	1	0.0786
	188	62	75.8	1.17	0.78	12.94	0.0276	1	0.153
	189	63	76.3	1.17	···	13.14	0.0255	1	0.141
	190	64	76.7	1.17	0.78	11.65	0.0466	1	0.258
	191	65	77.0	1.16	···	11.52	0.0493	1	0.274
	192	66	77.3	1.16	0.77	9.94	0.103	1	0.570
	193	67	77.7	1.16	···	10.01	0.0995	1	0.552

[a] Silicon taken as 10^6 atoms.

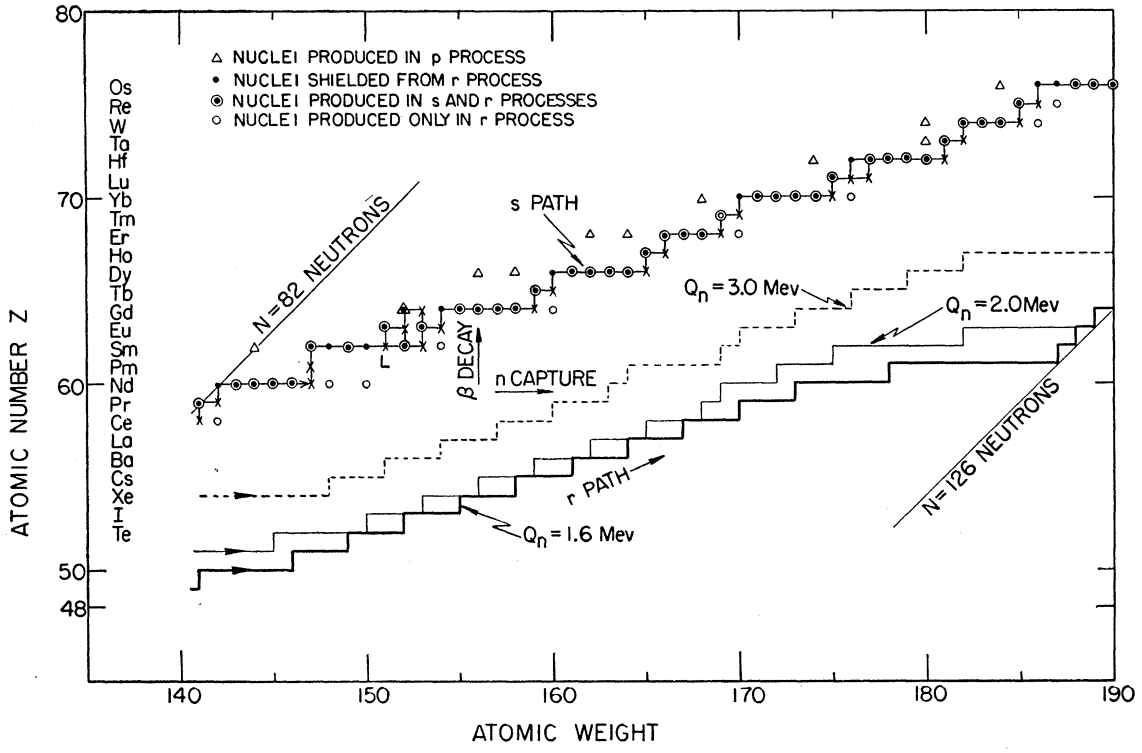

FIG. 3. Capture paths in the *r* process for different choices of critical neutron-binding energy. The symbol *L* denotes a lifetime longer than the time scale of the *s* process.

nuclei in nature, but are off the *s*-capture "path," and so are produced *only* in the *r* process. The open circles (even A) and plus-signs (odd A) represent nuclei produced predominantly by the *r* process. The *s* process contributes very little in this range of elements owing to the large size of the neutron capture cross sections of these nuclei. The most probable path of the *r* process for $Q_n \geqslant 1.6$ Mev is shown, along with that for the *s* process, in Fig. 3.

The effect of shell closure and spheroidal deformation on the abundance distribution may be seen by comparing Figs. 1 and 2. Large abundance will be associated with stability against neutron capture, that is, with low neutron capture energies; similarly, small abundances will be associated with high neutron capture energies. Immediately following shell closure at $N=82$, there is a rapid rise in neutron binding energy until $N\sim100$. This produces the minimum in $n(A)$ near $A=145$. From $N=100$ to 114 there is a minimum in neutron binding energy, producing the maximum in abundances between $A=146$ and 174. From $N=114$ to 126, there is again a rapid rise in binding energy, resulting in another abundance minimum between $A=174$ and 186. The rise in $n(A)$ beyond this point is because of shell closure at 126 neutrons. The behavior between 82 and 126 neutrons is quite similar to that found in the work of BBFH for nuclei containing more than 126 neutrons, and supports their view of the enhanced production of Th^{232}, U^{235}, U^{238}, Cf^{254}, etc., because of such deformation beyond $N=126$.

Effect of T_9 and n_n on the Capture Path

Equation (1) is illustrated in Fig. 4 with T_9 plotted against the critical neutron-binding energy Q_n for several values of the neutron density n_n. Clearly, the effect on Q_n of elevating the temperature, meanwhile holding the neutron density fixed, is similar to that obtained by decreasing n_n but keeping T_9 constant. The light line in Fig. 2 is the result of a choice of 2.0 Mev for Q_n. If n_n is taken as 10^{24} neutrons/cm^3, it represents a temperature of 1.0×10^9 degrees Kelvin, as compared with 0.8×10^9 for the heavy line (for which $Q_n=1.6$ Mev). Alternatively, both abundance curves could represent a common temperature but differing conditions of neutron density. Physically, this is not difficult to understand. An increase in the temperature increases the number of high-energy quanta, thereby aiding photoejection of neutrons. Similarly, decreasing the neutron density, meanwhile holding the temperature fixed, decreases the rate of neutron capture, thus providing less competition with photoejection. The critical value of Q_n above which neutron capture proceeds would be elevated in both cases.

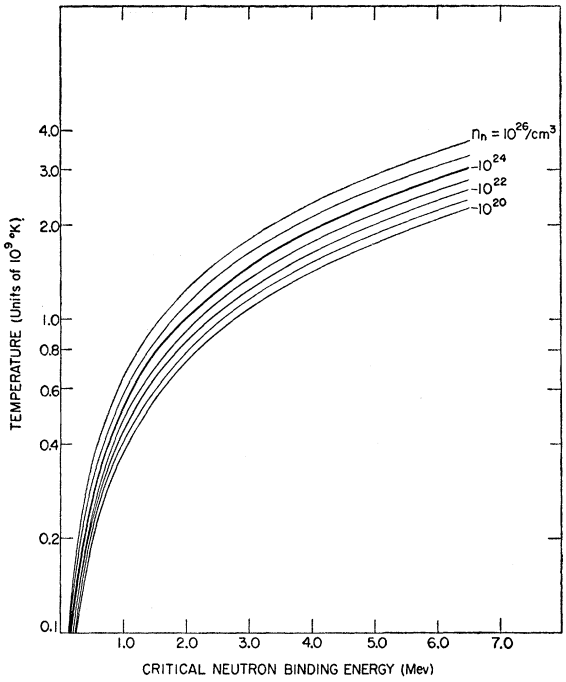

FIG. 4. Temperature against critical neutron-binding energy for several values of the neutron density.

Referring again to Fig. 3, the rapid-capture paths for $Q_n=1.6$ Mev and for $Q_n=2.0$ Mev may be compared. On the average, the path $Q_n=2.0$ Mev passes through neutron-rich nuclei for which $Z-Z_A$ is less than for those along the path $Q_n=1.6$ Mev. Assuming that the decay energy W_β is linearly proportional to $Z-Z_A$, and that the mean lifetime varies as W_β^{-5}, an appreciable difference in abundances can be expected between the two cases. For further comparison, the path appropriate to $Q_n=3.0$ Mev ($T_9\simeq 1.5$ at $n_n=10^{24}$) is also shown dashed in the figure.

Points Requiring Further Investigation

An abstract of this material was presented at the Los Angeles meeting of the American Physical Society in December, 1958. At that time, attention was called to the possible disagreement for the rare-earth abundances in the region of $A=165$ to 175. We still find this effect in the present calculations using the best choice of Q_n, namely, 1.6 Mev. This is seen in Fig. 2, where the calculated histogram lies above the SU points in the range $A=165$ to 175. However, we hesitate to regard the deviation as significant since the shape of the histogram in this region depends on the exact location of the valley in the excess neutron binding energy near $N=112$ (see Fig. 1). This depends both on the accuracy of the empirical mass differences and on the choice of the constant β employed in the calculations. Further, the exact location of the abundance minimum near $A=185$ of the histogram in Fig. 2 depends to some extent on the choice of the critical neutron binding energy. Finally, a better fit in the region $A=140$ to 185 could probably be obtained by lowering the calculated curve, i.e., by changing the normalization procedure or by ignoring the factor of two arising from cycling after fission. All of these details are being investigated further.

Other details deserving of additional study are improved modification of the mass formula and possible inaccuracies which become pronounced for large displacements from the stability region. In particular, it will be important to investigate the effect of retaining a surface×isotopic asymmetry term in the smooth Weizsäcker formula.

ACKNOWLEDGMENTS

R. A. Becker wishes to express his appreciation for the support by the John Simon Guggenheim Memorial Foundation and to the gracious hospitality extended him by the California Institute of Technology.